Dopamine D_2-like receptors selectively block N-type Ca^{2+} channels to reduce GABA release onto rat striatal cholinergic interneurones

Toshihiko Momiyama *† and Eiko Koga †

Division of Cerebral Structure, National Institute for Physiological Sciences, Myodaiji, Okazaki 444-8585 and † Department of Physiology, Nagasaki University School of Medicine, Sakamoto, Nagasaki 852-8523, Japan

1. The modulatory roles of dopamine (DA) in inhibitory transmission onto striatal large cholinergic interneurones were investigated in rat brain slices using patch-clamp recording.

2. Pharmacologically isolated $GABA_A$ receptor-mediated IPSCs were recorded by focal stimulation within the striatum. Bath application of DA reversibly suppressed the amplitude of evoked IPSCs in a concentration-dependent manner (IC_{50}, 10.0 μM).

3. A D_2-like receptor agonist, quinpirole (3–30 μM), also suppressed the IPSCs, whereas a D_1-like receptor agonist, SKF 81297, did not affect IPSCs. Sulpiride, a D_2-like receptor antagonist, blocked the DA-induced suppression of IPSCs (apparent dissociation constant (K_B), 0.36 μM), while a D_1-like receptor antagonist, SCH 23390 (10 μM), had no effect.

4. DA (30 μM) reduced the frequency of spontaneous miniature IPSCs (mIPSCs) without changing their amplitude distribution, suggesting that GABA release was inhibited, whereas the sensitivity of postsynaptic $GABA_A$ receptors was not affected. The effect of DA on the frequency of mIPSCs was diminished when extracellular Ca^{2+} was replaced by Mg^{2+} (5 mM), indicating that DA affected the Ca^{2+} entry into the presynaptic terminal.

5. An N-type Ca^{2+} channel selective blocker, ω-conotoxin GVIA (ω-CgTX, 3 μM), suppressed IPSCs by 65.4 %, whereas a P/Q-type Ca^{2+} channel selective blocker, ω-agatoxin IVA (ω-Aga-IVA, 200 nM), suppressed IPSCs by 78.4 %. Simultaneous application of both blockers suppressed IPSCs by 95.9 %. Assuming a 3rd power relationship between Ca^{2+} concentration and transmitter release, the contribution of N-, P/Q- and other types of Ca^{2+} channels to presynaptic Ca^{2+} entry is estimated to be, respectively, 29.8, 40.0 and 34.5 % at this synapse. After the application of ω-CgTX, DA (30 μM) no longer affected IPSCs. In contrast, ω-Aga-IVA did not alter the level of suppression by DA, suggesting that the action of DA was selective for N-type Ca^{2+} channels.

6. A G protein alkylating agent, *N*-ethylmaleimide (NEM), significantly reduced the DA-induced suppression of IPSCs.

7. These results suggest that presynaptic D_2-like receptors are present on the terminals of GABAergic afferents to striatal cholinergic interneurones, and down-regulate GABA release by selectively blocking N-type Ca^{2+} channels through NEM-sensitive G proteins.

Large cholinergic neurones in the striatum are interneurones and are the primary source of acetylcholine (ACh) in the basal ganglia (Bolam *et al.* 1984; Phelps *et al.* 1985). These neurones are one of the targets of dopaminergic terminals from the substantia nigra pars compacta (Kubota *et al.* 1987). Modulation of excitability of these neurones by dopamine (DA) is important, since it has been proposed in many studies that the balance between DA and ACh is essential for motor control, and disruption of this balance could lead to the dysfunction

observed in Parkinson's disease (Lehmann & Langer, 1983; Calabresi *et al.* 2000; Kaneko *et al.* 2000). Striatal cholinergic neurones express both D_1-like and D_2-like DA receptors (Kawaguchi *et al.* 1995; Bergson *et al.* 1995; Yan & Surmeier, 1997). Several studies have reported DA receptor-mediated modulation of voltage- or ligand-gated ion channels on these neurones. For example, activation of postsynaptic D_1-like receptors excites rat striatal cholinergic neurones in slices by suppressing the resting K^+ conductance or opening a non-selective cation

conductance (Aosaki *et al.* 1998), whereas activation of D_2-like receptors in dissociated striatal cholinergic neurones reduces N-type Ca^{2+} currents (Yan *et al.* 1997). As for the ligand-gated channels, various different $GABA_A$ receptor subunits are coexpressed in acutely dissociated striatal cholinergic neurones and their Zn^{2+}-sensitive component is reported to be enhanced via D_1-like (D_5) receptors (Yan & Surmeier, 1997). However, it is not yet clear if the same receptor subtype operates at GABAergic synapses derived predominantly from striatal medium spiny neurones (Bolam *et al.* 1986; Martone *et al.* 1992; Bennett & Wilson, 1998, 1999). Compared to the postsynaptic DA receptor actions, little information has been available on the modulation of synaptic transmission onto striatal cholinergic neurones. Recently, using the conventional microelectrode recording, inhibition of $GABA_A$ receptor-mediated postsynaptic potentials via D_2-like receptors was reported in striatal cholinergic neurones (Pisani *et al.* 2000). However, the detailed mechanism underlying the DA-induced modulation of GABAergic transmission onto these neurones still remains to be elucidated. The aim of the present study was to investigate this mechanism by whole-cell patch-clamp recording in a thin-slice preparation of the rat brain. This technique allows resolution of quantal synaptic responses recorded as miniature synaptic currents, whose frequency and amplitude reflect pre- and postsynaptic changes, respectively. We have made use of this analysis to identify the site of action of DA and we also identified the specific Ca^{2+} channel subtype and the class of G proteins involved in the modulation of GABAergic transmission by DA.

Preliminary data from the present study have been published in an abstract form (Momiyama & Koga, 1999).

METHODS

Slice preparation

All experiments were carried out according to the Guiding Principles for the Care and Use of Animals in the Field of Physiological Sciences of Physiological Society of Japan (1998). Standard artificial cerebrospinal fluid (aCSF) had the following composition (mM): NaCl, 124; KCl, 3; $CaCl_2$, 2.4; $MgCl_2$, 1.2; NaH_2PO_4, 1; $NaHCO_3$, 26; D-glucose, 10; pH 7.4 adjusted by 95% O_2–5% CO_2. Neonatal rats (12–20 days old) were decapitated under deep ether anaesthesia, and coronal slices (200 μm) containing the striatum were cut using a microslicer (DTK-1000, DOSAKA, Kyoto, Japan) in ice-cold oxygenated low-Ca^{2+} (0.5 mM), high-Mg^{2+} (6 mM) aCSF. The slices were then transferred to a holding chamber containing standard aCSF solution. Slices were incubated in the holding chamber maintained at room temperature (21–25 °C) for at least 1 h before recording.

Whole-cell recording and data analysis

For recording, a slice was transferred to the recording chamber, held submerged, and superfused continuously with the aCSF (bubbled with 95% O_2–5% CO_2) at a rate of 4–5 ml min^{-1}.

Patch electrodes were pulled from standard-walled borosilicate glass capillaries (1.5 mm outer diameter; Clark Electromedical, Reading,

UK) and had resistances of 2.5–6 MΩ when filled with a caesium chloride-based internal solution of the following composition (mM): CsCl, 140; NaCl, 9; Cs-EGTA, 1; Cs-Hepes, 10; Mg-ATP, 2 (pH adjusted with 1 M CsOH). Whole-cell recordings were made using a patch-clamp amplifier (Axopatch 1D or Axopatch 200B, Axon Instruments, Foster City, CA, USA). The cell capacitance and the series resistance were measured from the amplifier. The access resistance was monitored by measuring capacitative transients obtained in response to a hyperpolarizing voltage step (5 mV, 25 ms) from a holding potential of −60 mV. No correction was made for the liquid junction potential (calculated to be 5.0 mV by pCLAMP7 software, Axon Instruments). To evoke synaptic currents, voltage pulses (0.2–0.4 ms in duration) of suprathreshold intensity were delivered at 0.2 Hz extracellularly via a stimulating electrode filled with 1 M NaCl placed within a 50–120 μm radius (mean distance $77 \pm 2.0\ \mu$m, $n = 115$) of the recorded neurone. The position of the stimulating electrode was varied until a stable response was evoked in the recorded cell. All the inhibitory postsynaptic currents (IPSCs) were recorded at a holding potential (V_h) of −60 mV. Experiments were carried out at room temperature (21–25 °C).

Data were stored on digital-audio tapes using a DAT recorder (DTR-1204, Biologic, France, DC to 10 kHz). IPSCs were digitized off-line at 10 kHz (low-pass filtered at 2 kHz with an 8-pole Bessel filter) using pCLAMP6 or pCLAMP7 (Axon Instruments) software. The effects of DA or DA receptor agonists on the evoked IPSCs were assessed by averaging IPSC amplitudes for 100 s (20 traces) during the peak response to the drug and comparing this value with the averaged amplitude of 20 traces just before drug application. Miniature IPSCs (mIPSCs) were filtered at 2 kHz and digitized at 20 kHz using Axotape (Axon Instruments) software and analysed using N software (provided by Dr S. F. Traynelis, Emory University). The effect of DA on mIPSCs was assessed by comparing the frequency and amplitude distribution of the events for 5–10 min during the peak response to DA with those obtained just before DA application. The concentration–response curve was fitted to the theoretical equation:

$$Y = A\left(1 - \frac{1}{1 + (X/X_0)^n}\right),$$

where Y is the percentage inhibition of IPSCs, X is the concentration of DA, A is the maximal percentage inhibition of IPSCs, X_0 is the IC_{50}, and n is the Hill slope. The fitting was done using the embedded logistic function in Origin (Microcal Software, Northampton, MA, USA). An apparent dissociation constant (K_B) for sulpiride, a D_2-like receptor antagonist, was calculated using the equation:

$$K_B = [B]/(DR - 1),$$

where [B] is the concentration of sulpiride and DR (dose ratio) is the ratio of IC_{50} values for pooled data observed in the presence and absence of the antagonist, assuming that sulpiride behaves as a competitive antagonist. Statistical analysis was carried out using both Student's *t* test (two-tailed) and a non-parametrical Mann-Whitney *U* test. The Kolmogorov-Smirnov (K-S) test was used for the comparison of cumulative probability distributions of mIPSCs. In all statistics, 0.05 was used as the confidence limit. Data are expressed as means $\pm$ S.E.M.

Drugs

Drugs were stored as frozen stock solutions and dissolved in the perfusate at the final concentration just prior to use. ($\pm$)-6-Chloro-7,8-dihydroxy-1-phenyl-2,3,4,5-tetrahydro-1H-3-benzazepine hydrobromide (SKF 81297), *trans*-(−)-4aR-4,4a,5,6,7,8,8a,9-octa-hydro-5-propyl-1H-pyrazolo[3,4-g]quinoline hydrochloride (quinpirole), $R(+)$-7-chloro-8-hydroxy-3-methyl-1-phenyl-2,3,4,5-tetrahydro-1H-3-benzazepine hydrochloride (SCH 23390), and $S(-)$-5-amino-

sulfonyl-*N*-[(1-ethyl-2-pyrrolidinyl)-methyl]-2-methoxybenzamide (sulpiride) were purchased from Research Biochemicals International (Natick, MA, USA). 6-Cyano-7-nitroquinoxaline-2,3-dione (CNQX), D(−)-2-amino-5-phosphonopentanoic acid (D-AP5) and 1-(2-bis(4-fluoro-phenyl)methoxy)ethyl)-4-(3-phenylpropyl)piperazine dihydrochloride (GBR 12909) were purchased from Tocris Cookson (Bristol, UK), dopamine, bicuculline methochloride, strychnine and *N*-ethylmaleimide (NEM) from Sigma (St Louis, MO, USA), tetrodotoxin (TTX) from Sankyo (Tokyo, Japan), and synthetic ω-conotoxin GVIA (ω-CgTX) and ω-agatoxin IVA (ω-Aga-IVA) from Peptide Institute (Osaka, Japan). To prevent oxidative degradation of dopamine, sodium metabisulfite (50 μM, Sigma) was always added to dopamine-containing solutions. Sodium metabisulfite alone had no effect on the IPSCs or the holding current. ω-CgTX and ω-Aga-IVA were dissolved in oxygenated aCSF containing cytochrome *c* (1 mg ml^{-1}; Sigma).

Identification of cholinergic neurones in the striatum

Neurones in the striatum were viewed with a microscope fitted with a water-immersion optic (Nikon, Tokyo, Japan or Olympus BX50WI, Olympus, Tokyo, Japan). Only those within the dorsal part of the striatum were used in the present study (Fig. 1*A*). Large neurones whose somatic diameter of the long axis was greater than 30 μm (Fig. 1*B* and *C*) were selected for whole-cell recording according to the size distribution of cholinergic and non-cholinergic neurones in the striatum (Kawaguchi, 1992). The mean somatic diameter of the long axis was 36.7 $\pm$ 0.22 μm ($n = 146$). In order to functionally identify striatal cholinergic neurones, the membrane properties of these large cells were also examined (Fig. 1*D*). Hyperpolarizing current pulses were applied through the recording pipette (containing Cs$^+$ to block the inwardly rectifying K$^+$ conductance) under current-clamp mode, and neurones that exhibited a characteristic voltage sag during a large
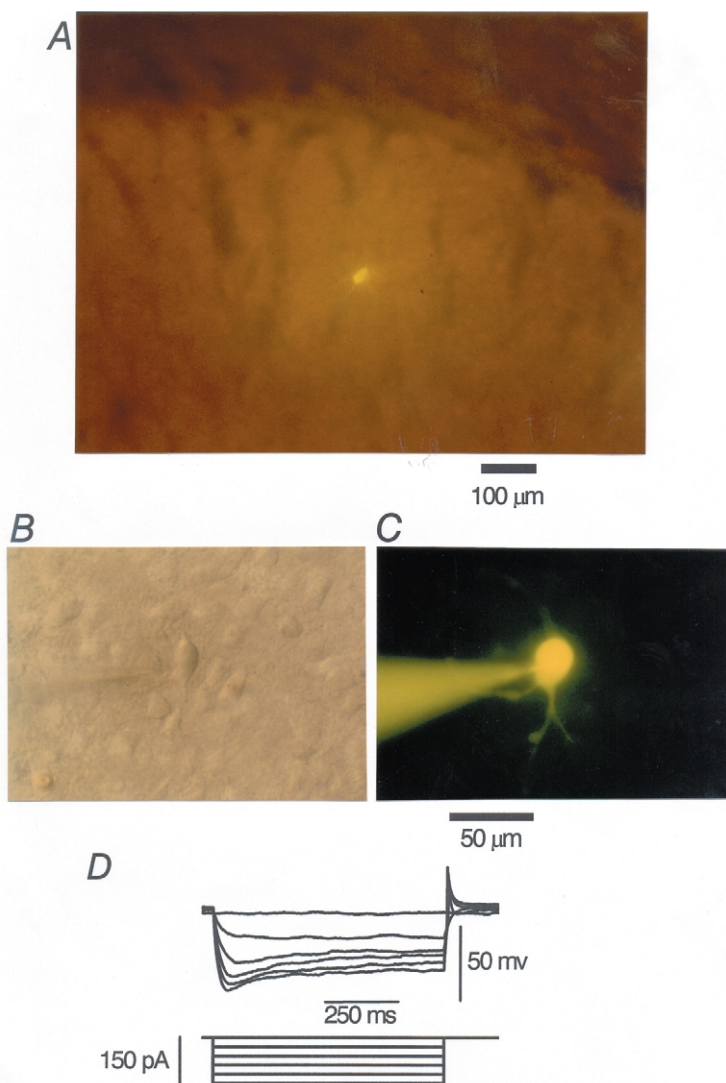
Figure 1. Identification of striatal cholinergic neurones

A, a striatal cholinergic neurone filled with Lucifer Yellow (0.1 %) in the dorsolateral striatum in a coronal slice (17-day-old rat). The dorsal side is at the top and the lateral side is to the right. *B*, Nomarski view of another striatal cholinergic neurone at a higher magnification. *C*, the neurone in *B* filled with Lucifer Yellow. Scale bar applies to both *B* and *C*. *D*, membrane potentials recorded from another large striatal neurone in response to hyperpolarizing current pulses applied intracellularly through Cs$^+$-filled electrodes. Voltage sags during hyperpolarizing current pulses, characteristic of striatal cholinergic neurones, were identified.

hyperpolarization (Jiang & North, 1991; Kawaguchi, 1992; Kawaguchi *et al.* 1995; Aosaki *et al.* 1998) were chosen (Fig. 1*D*) and used for the present study. The cell capacitance was 43.9 ± 0.72 pF ($n = 149$) and series resistance was 12.8 ± 0.28 MΩ ($n = 149$).

RESULTS

Identification of GABAergic IPSCs in striatal cholinergic interneurones

Synaptic currents were evoked at a holding potential (V_h) of -60 mV by focal stimulation in the presence of CNQX (5 μM), D-AP5 (25 μM) and strychnine (0.5 μM) to block glutamatergic and glycinergic components. Under these conditions, the mean amplitude of the evoked synaptic currents was -217.7 ± 16.2 pA ($n = 115$). These synaptic currents were reversibly blocked by bicuculline (10 μM) (Fig. 2*B*) in all of the 12 neurones examined, confirming that they were mediated by GABA$_A$ receptor channels. As expected for GABAergic IPSCs, the synaptic currents reversed close to the estimated equilibrium potential of chloride ions (Fig. 2*A*). Thus in subsequent experiments, GABAergic IPSCs were pharmacologically isolated using the same combination of blockers.

Suppression of the evoked IPSCs by DA

Bath application of DA (30 μM) reversibly suppressed the amplitude of IPSCs as shown in Fig. 3*A*. The suppression reached steady state within a few minutes, and IPSCs

recovered after 5–10 min of washout (Fig. 3*A*). The inhibitory effect of DA (30 μM) was reproduced upon repeated application (6 cells, data not shown). In all cholinergic neurones examined (89 cells) DA exhibited a concentration-dependent inhibitory effect on IPSCs at concentrations between 0.3 and 1000 μM. Figure 3*B* depicts the concentration dependence of the DA effect, giving an apparent IC$_{50}$ value, maximum IPSC depression and Hill slope value of 10.0 μM, 65.4% and 1.1, respectively.

The existence of a dopamine transporter (DAT) in the dorsolateral striatum of adult rats has been reported by Nirenberg *et al.* (1996). If DAT is already expressed at the postnatal stage of the animals used in the present study, exogenously applied DA may be taken up and the apparent affinity of DA could be underestimated. To investigate this possibility, we next examined the effect of a DA uptake inhibitor, GBR 12909. After confirming the recovery of IPSCs from DA-induced inhibition, GBR 12909 (10 μM) was applied for 5–7 min, and then DA was applied again in the presence of GBR 12909. GBR 12909 alone had no effect on the amplitude of evoked IPSCs (96.2 $\pm$ 3.9%, $n = 8$, $P > 0.05$). As summarized in Fig. 3*C*, GBR 12909 significantly enhanced the degree of inhibition of IPSCs by 3 μM DA ($n = 4$). However, when the concentration of DA was raised to 30 μM, GBR 12909
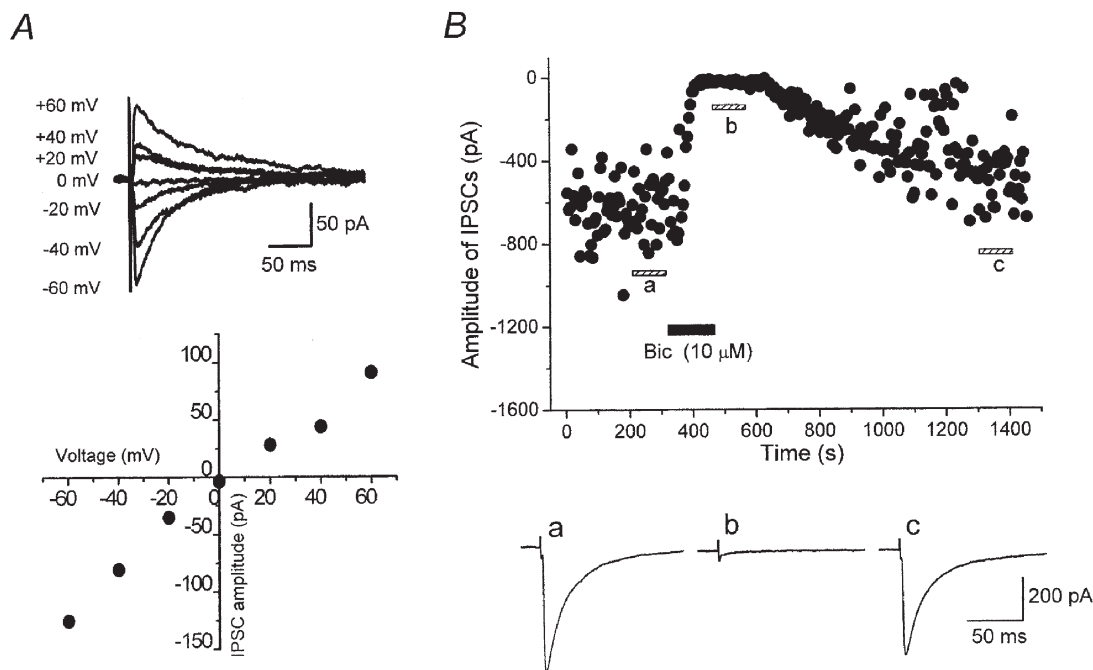
Figure 2. Characteristics of GABAergic inhibitory postsynaptic currents (IPSCs) recorded in striatal cholinergic neurones

A, current–voltage (*I–V*) relationship of IPSCs evoked at 0.2 Hz in the presence of CNQX (5 μM), D-AP5 (25 μM) and strychnine (0.5 μM). Average traces of 10 IPSCs at each potential are shown, and the peak current magnitude is plotted against V_h. IPSCs reversed at potential close to the Cl$^-$ equilibrium potential E_{Cl} (+2.6 mV). The holding current was -22 pA at -60 mV. *B*, IPSCs were blocked by bath-applied bicuculline (Bic, 10 μM). The amplitude of IPSCs evoked at 0.2 Hz is plotted against time. Traces *a–c* are averages of 20 consecutive IPSCs during the indicated periods.

no longer affected the inhibitory effect of DA ($n = 4$), suggesting that the endogenous DA uptake system was saturated at higher DA concentrations. In the present study, we did not observe any postsynaptic effect of DA upon holding currents or membrane conductances. A previous study by Aosaki *et al.* (1998) reported that the activation of the postsynaptic D_1-like receptors of striatal cholinergic neurones caused excitation via a G protein-dependent pathway. Because we used a CsCl-based GTP-free internal solution in all experiments, such postsynaptic effects would be blocked.

Pharmacological identification of DA receptor subtypes

In order to identify which DA receptor subtype mediates DA-induced inhibition of IPSCs, the effects of selective DA receptor agonists (Fig. 4) and antagonists (Fig. 5) were further examined. Firstly, the effects of a selective D_1-like receptor agonist, SKF 81297 (30 μM), and a selective D_2-like receptor agonist, quinpirole (3 and 30 μM), on the amplitude of IPSCs were compared with those of DA (Fig. 4). Quinpirole at concentrations of 3 and 30 μM inhibited IPSCs by $34.1 \pm 6.6\%$ ($n = 4$) and $55.8 \pm 5.6\%$ ($n = 9$), respectively. The effect of 3 μM quinpirole was

significantly ($P < 0.05$) larger than that of DA at the same dose ($11.2 \pm 2.7\%$, $n = 13$), but not significantly ($P > 0.05$) different from that in the presence of the DA uptake inhibitor GBR 12909 ($31.4 \pm 6.2\%$, $n = 4$), probably because quinpirole is not a substrate for uptake. The effect of 30 μM quinpirole was not significantly ($P > 0.05$) different from that of 30 μM DA ($48.6 \pm 1.7\%$, $n = 46$), in agreement with the interpretation proposed above that the uptake carrier was saturated at higher DA concentrations. In contrast, SKF 81297 (30 μM) did not significantly affect IPSCs ($91.2 \pm 5.9\%$ of control, $n = 9$, $P > 0.05$). Therefore it is suggested that the action of DA is mediated by D_2-like receptors. To test this possibility further, the effects of a D_1-like receptor antagonist, SCH 23390, and a D_2-like receptor antagonist, sulpiride, were investigated. As shown in Fig. 5, after confirming the effect of DA and recovery on washout, the antagonist was applied for at least 7 min, and then DA was applied again in the presence of the antagonist. Application of SCH 23390 (10 μM) or sulpiride (5 μM) itself had no effect on the IPSCs in any of 22 or 20 neurones tested, respectively. As expected, sulpiride antagonized the DA-induced inhibition of IPSCs (Fig. 5*B*). The concentration–response curve for DA was shifted to the right in the
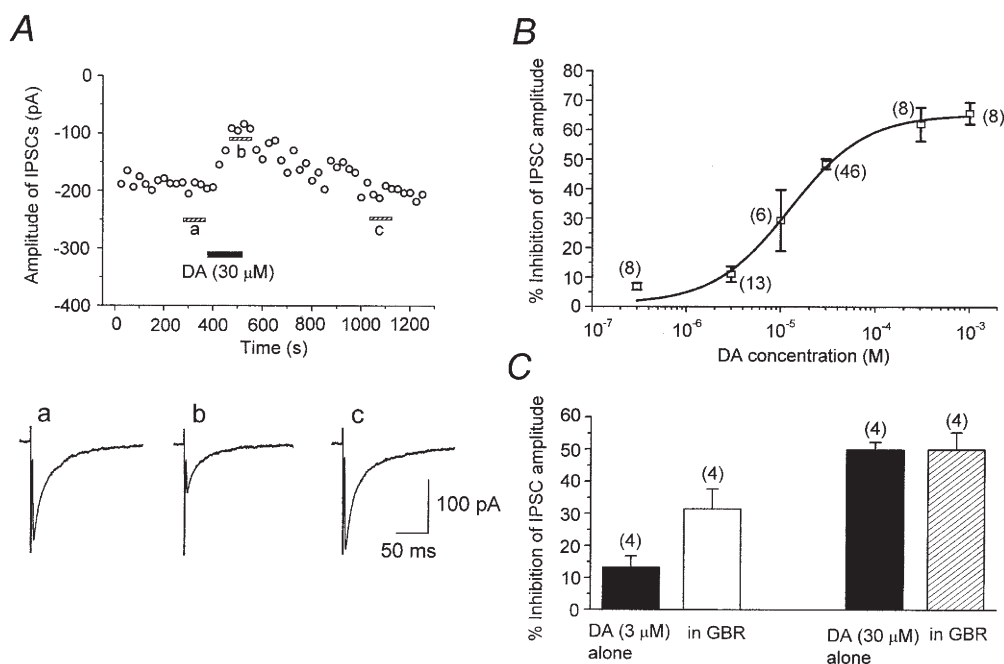
Figure 3. Inhibition of GABAergic IPSCs by dopamine (DA)

IPSCs were evoked at 0.2 Hz. V_h, -60 mV. *A*, time course of the inhibitory effect of DA (30 μM) on the amplitude of evoked IPSCs. Each point represents the mean amplitude of five consecutive responses. DA was bath applied during the indicated period. The traces *a–c* show averages of 20 consecutive IPSCs during the indicated periods. *B*, concentration-dependent inhibition of IPSCs by DA. Numbers of cells are shown in parentheses. Error bars indicate S.E.M. The data were fitted to a logistic function (superimposed curve; see Methods) to estimate the IC_{50} value (10.0 μM), maximum inhibition (by 65.4%) and Hill slope (1.1). *C*, effect of the endogenous DA uptake system upon DA-induced suppression of IPSCs. For the same cell (numbers of cells shown in parentheses), the effect of DA (3 and 30 μM) was examined in the absence and presence of the DA uptake inhibitor GBR 12909 (GBR, 10 μM). GBR significantly enhanced the action of DA at 3 μM, but not at 30 μM.

presence of sulpiride, with an IC_{50} value of 150 μM (Fig. 5*B*). From this shift, an apparent K_B value for sulpiride was calculated to be 0.36 μM (pK_B 6.4). On the other hand, SCH 23390 did not affect the concentration–response curve for the effect of DA, with an estimated IC_{50} value of 7.8 μM (10.0 μM in the case of DA alone) (Fig. 5*A*), supporting the lack of involvement of D_1-like receptors.

Effect of DA on miniature IPSCs

In order to dissect out the site of action of DA, the effects of DA on the frequency and amplitude of miniature IPSCs (mIPSCs) were examined (Koga & Momiyama, 2000). Spontaneous GABAergic mIPSCs were recorded from striatal cholinergic interneurones in the presence of TTX (0.3 μM) as well as CNQX (5 μM), D-AP5 (25 μM) and strychnine (0.5 μM). These mIPSCs were reversibly blocked by bicuculline (10 μM, Fig. 6*A*) in all of the five neurones tested, indicating that they were GABAergic mIPSCs. The occurrence of mIPSCs (0.29 $\pm$ 0.05 Hz, $n = 8$, in a standard external Ca^{2+} concentration of 2.4 mM) was clearly dependent on Ca^{2+} entry to presynaptic terminals, since replacement of external Ca^{2+} with Mg^{2+} (5 mM) reduced the frequency of mIPSCs to 0.12 $\pm$ 0.02 Hz ($n = 8$). In 2.4 mM Ca^{2+}, application of DA (30 μM) reduced the frequency of mIPSCs, and the effect reached a steady state within 3 min (Fig. 6*B*). Figure 6*C* and *D* shows the cumulative probability distributions (and frequency distributions; insets) for the DA-induced

effects on mIPSC inter-event intervals (Fig. 6*C*) and amplitude (Fig. 6*D*). As is clear from these plots, DA caused a shift in the inter-event interval distribution toward longer intervals (i.e. lower frequencies), without changing the amplitude distribution. DA significantly shifted the inter-event intervals ($P < 0.05$, K-S test) in all of the eight neurones tested, whereas the amplitude distribution was not affected by DA in any of the eight neurones ($P > 0.05$, K-S test). The average reduction in the frequency of mIPSCs was 47.2 $\pm$ 2.4 % ($n = 8$, Fig. 7*D*). However, the mean amplitude of mIPSCs (28.5 $\pm$ 4.5 pA, $n = 8$) was not affected by DA (101 $\pm$ 3.4 % of control, $n = 8$), as shown in Fig. 6*E*. These results suggest that DA reduced the GABA release from presynaptic terminals, without affecting the sensitivity of postsynaptic $GABA_A$ receptors.

In order to determine whether the presynaptic action of DA is targeted at Ca^{2+} entry or the release machinery itself, we next examined the effect of DA in nominally Ca^{2+}-free solution. As shown in Fig. 7, DA (30 μM) no longer affected the frequency of mIPSCs (Fig. 7*A* and *D*, 94.4 $\pm$ 2.4 % of control, $n = 7$). In all seven neurones examined, DA in nominally Ca^{2+}-free solution did not change the distributions of inter-event intervals (Fig. 7*B*) or amplitudes (Fig. 7*C*). The mean amplitude of mIPSCs was also unaffected by DA (99.5 $\pm$ 6.1 % of control, $n = 7$). These results suggest that DA reduced Ca^{2+} entry into presynaptic terminals, thereby suppressing GABA release.
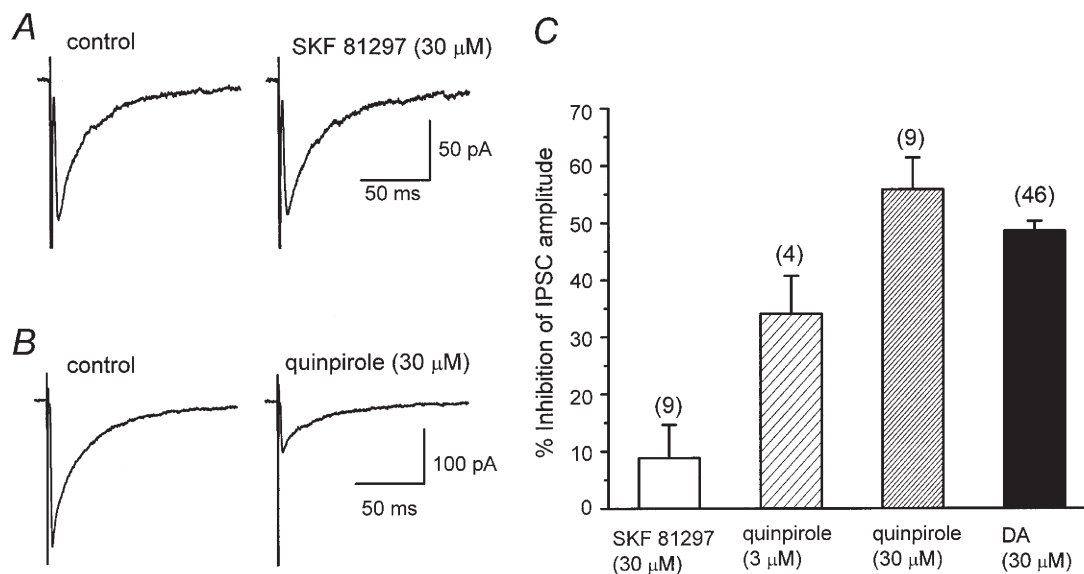
Figure 4. Effect of DA receptor agonists on evoked IPSCs
All IPSCs were evoked at 0.2 Hz. V_h, -60 mV. *A*, lack of effect of a D_1-like receptor agonist, SKF 81297 (30 μM). *B*, inhibitory effect of a D_2-like receptor agonist, quinpirole (30 μM). Each trace is the average of 20 IPSCs. *C*, histograms summarizing the mean inhibitory effect of SKF 81297 (30 μM), quinpirole (3 and 30 μM) and DA (30 μM). Error bars indicate S.E.M. Values for SKF 81297, 3 μM quinpirole, 30 μM quinpirole and DA were 8.8 $\pm$ 5.9 % ($n = 9$), 34.1 $\pm$ 6.6 % ($n = 4$), 55.8 $\pm$ 5.6 % ($n = 9$) and 48.6 $\pm$ 1.7 % ($n = 46$), respectively. The effects of 30 μM quinpirole and 30 μM DA were not significantly different ($P > 0.05$).

Identification of presynaptic Ca²⁺ channel subtype coupled with the inhibitory action of DA

In the CNS, fast synaptic transmission is governed by multiple types of Ca^{2+} channels (Takahashi & Momiyama, 1993; Wheeler *et al.* 1994). In order to identify which Ca^{2+} channel subtype is involved in the suppression of IPSCs by presynaptic D_2-like receptors, the effects of ω-CgTX, the N-type Ca^{2+} channel selective blocker, and ω-Aga-IVA, the P/Q-type Ca^{2+} channel selective blocker, were examined.

Firstly, we examined the relative contribution of different Ca^{2+} channel subtypes at this synapse. Bath application of ω-CgTX (3 μM) or ω-Aga-IVA (200 nM) caused a gradual decline in the amplitude of IPSCs, which reached a steady state in 5–10 min (Fig. 8*A* and *B*). The percentage inhibition induced by ω-CgTX was $65.4 \pm 3.3\%$ ($n = 11$) and that by ω-Aga-IVA was $78.4 \pm 2.7\%$ ($n = 7$, Fig. 8*D*). The effects of both toxins were irreversible. When both ω-CgTX and ω-Aga-IVA were applied, the degree of IPSC suppression was $95.9 \pm 1.5\%$ ($n = 6$, Fig. 8*C* and *D*). With regard to IPSC amplitude, there was an apparent overlap in the effects of ω-CgTX and ω-Aga-IVA. This overlap can be explained by the non-linear relationship between the presynaptic calcium concentration and the transmitter release described at various synapses (Jenkinson, 1957; Dodge & Rahamimoff, 1967; Augustine & Charlton, 1986; Takahashi, 1992; Takahashi & Momiyama, 1993): with such a non-linear relationship, only a small decrease in Ca^{2+} entry into presynaptic terminals would result in a large reduction in the synaptic currents. Assuming a power function for the relationship, the relative amplitude of postsynaptic currents remaining after application of ω-CgTX (A), ω-Aga-IVA (B) or both toxins (C) can be described as $A = (1 - a)^m$, $B = (1 - b)^m$ and $C = c^m$, where a, b and c represent a fraction of presynaptic Ca^{2+} channel subtypes sensitive to ω-CgTX (a) and ω-Aga-IVA (b) and those insensitive to these toxins (c), and m is the power coefficient (Takahashi & Momiyama, 1993). If each toxin at the present concentration selectively blocks only one presynaptic Ca^{2+} channel subtype, $a + b + c$ should be unity.
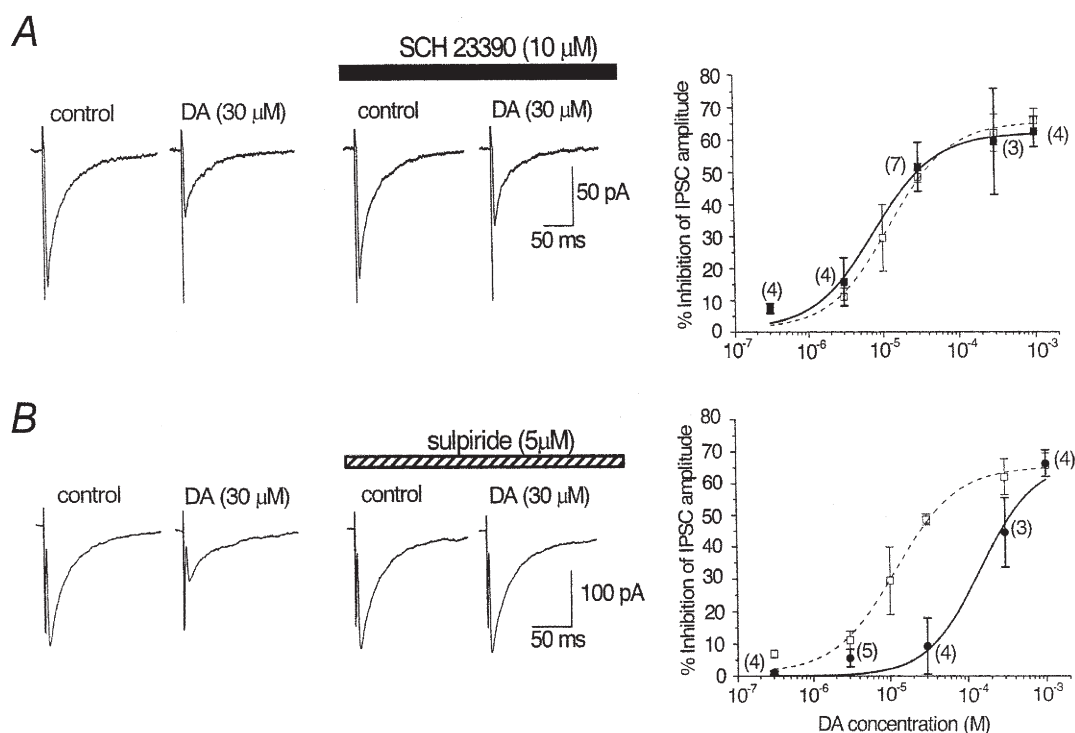
**Figure 5. Effects of DA receptor antagonists on DA-induced inhibition of evoked IPSCs**

Effects of DA on IPSCs (0.2 Hz; V_h, −60 mV) were compared in the absence and presence of a D_1-like receptor antagonist, SCH 23390 (10 μM; *A*), or a D_2-like receptor antagonist, sulpiride (5 μM; *B*). Traces are averages of 20 consecutive IPSCs. Antagonists were applied for 7 min before a second application of DA. The concentration of DA ranged from 0.3 μM to 1 mM and concentration–response curves in the absence (same as in Fig. 3*B*) and presence of each antagonist are superimposed in the graphs on the right. Error bars indicate S.E.M. and numbers of cells are given in parentheses. *A*, the concentration–response curve for IPSC inhibition remained unchanged by SCH 23390 (■) compared with the curve in the absence of SCH 23390 (□). The estimated IC₅₀ value, maximum inhibition and Hill slope were 7.8 μM, 62.0% and 1.1, respectively. *B*, the concentration–response curve was shifted to the right by sulpiride (●), with the estimated IC₅₀ value, maximum inhibition and Hill slope being 150 μM, 66.8% and 1.2, respectively. □, curve in the absence of sulpiride.

Assuming $m = 3$ or $m = 4$ (Dodge & Rahamimoff, 1967; Augustine & Charlton, 1986; Takahashi, 1992; Takahashi & Momiyama, 1993), the value was 1.04 ($a = 0.298$, $b = 0.400$, $c = 0.345$) or 1.00 ($a = 0.233$, $b = 0.318$, $c = 0.451$), respectively, supporting the idea that there was little overlap in terms of the Ca^{2+} channel subtype responsible for transmitter release.

After confirming DA (30 μM)-induced inhibition and recovery after washout, ω-CgTX (3 μM) was applied, and after the effect had reached a steady state, DA (30 μM) was applied again. DA (30 μM) no longer suppressed IPSCs in the presence of ω-CgTX (2.9 $\pm$ 1.4 % inhibition, $n = 5$, Fig. 9A and C). In contrast, in the presence of ω-Aga-IVA DA still suppressed IPSCs by 55.7 $\pm$ 7.6% ($n = 5$, Fig. 9B and C). The degree of the inhibitory action of DA on IPSCs, before and after the application of ω-Aga-IVA, was not significantly different ($P > 0.05$, Fig. 9C). These results indicate that the inhibitory action of DA was selectively coupled to presynaptic N-type Ca^{2+} channels.

Effect of NEM on DA-induced inhibition of evoked IPSCs

Previous studies in cell lines or dissociated neurones have demonstrated that activation of D_2-like receptors inhibits Ca^{2+} currents through pertussis toxin (PTX)-sensitive $G_{i/o}$ class G proteins (Lledo *et al.* 1992; Brown & Seabrook, 1995; Yan *et al.* 1997). To determine whether the present presynaptic D_2-like receptor-mediated effect also involves this class of G proteins, we examined the effect of the sulfhydryl alkylating agent N-ethylmaleimide (NEM), which disrupts coupling of PTX-sensitive $G_{i/o}$ type G proteins to Ca^{2+} channels (Shapiro *et al.* 1994). As shown in Fig. 10A, NEM (50 μM) alone had no effect on the evoked IPSCs. In the presence of NEM, DA (30 μM) exhibited only a small inhibitory effect (Fig. 10A). As shown in Fig. 10B, inhibition of IPSCs by DA was only 6.9 $\pm$ 5.2% ($n = 6$) in the presence of NEM, significantly smaller than that in the absence of NEM (44.3 $\pm$ 2.2%, $n = 6$, $P < 0.05$, Fig. 10B), indicating that NEM-sensitive G proteins are coupled to presynaptic D_2-like receptors.
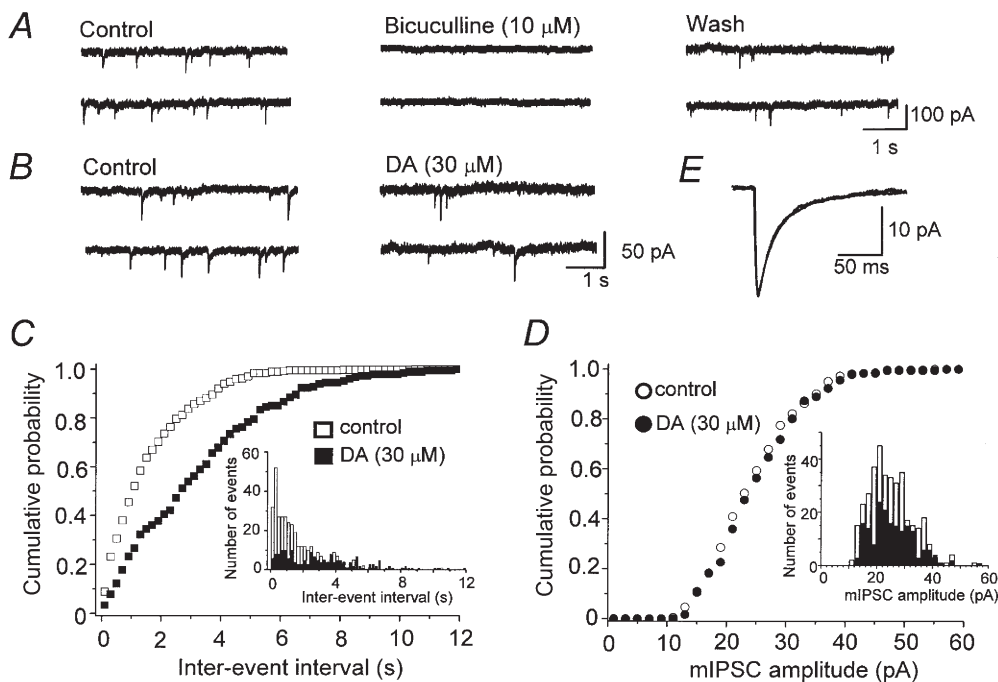
**Figure 6. Effect of DA on spontaneous miniature IPSCs (mIPSCs)**

The mIPSCs were recorded in the presence of TTX (0.3 μM), CNQX (5 μM), D-AP5 (25 μM) and strychnine (0.5 μM). V_h, -60 mV. A, consecutive traces recorded in control, 3 min after application of bicuculline (10 μM), and 15 min after washout. B, consecutive traces recorded before and 3 min after application of 30 μM DA. C and D, cumulative probability distribution of inter-event intervals (C) and peak amplitudes (D) of mIPSCs from the same neurone shown in B, comparing distributions in the absence (open symbols) and presence (filled symbols) of DA. Control data contain 364 events per 10 min period, and DA data contain 181 events per 10 min period. The inter-event interval was increased, whereas the mIPSC amplitude was unaffected by DA. Insets: histograms of inter-event intervals and amplitudes. E, superimposed traces of averaged mIPSCs in control (364 events) and during application of DA (181 events). The mean amplitudes of mIPSCs in control and in the presence of DA were 25.0 and 25.7 pA, respectively.
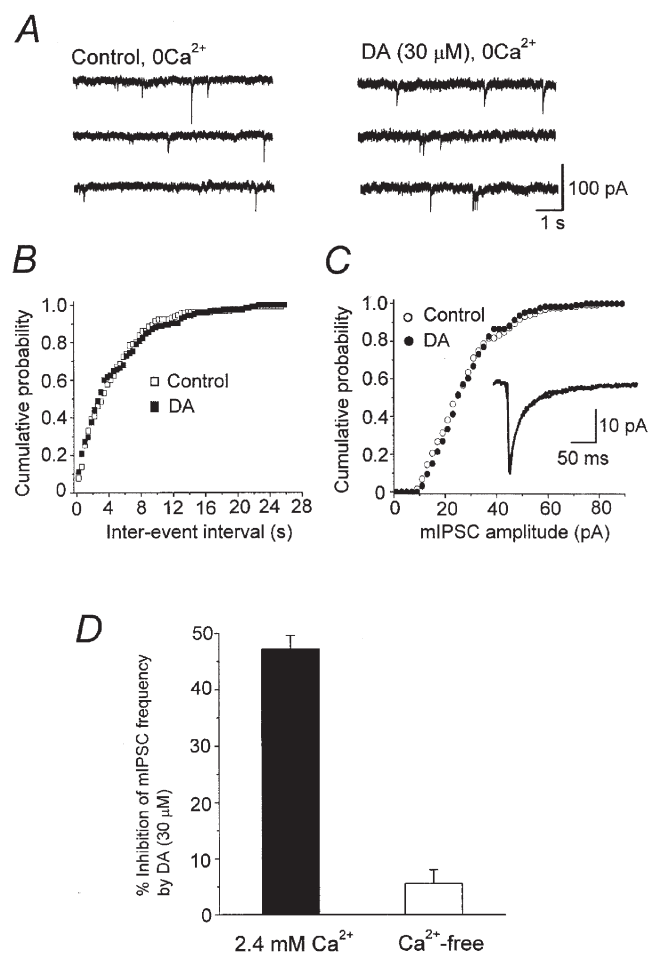
Figure 7. Lack of DA-induced effect on mIPSCs in Ca^{2+}-free solution

A, the mIPSCs were recorded in nominally Ca^{2+}-free, high-Mg^{2+} (5 mM) aCSF containing TTX (0.3 μM), CNQX (5 μM), D-AP5 (25 μM) and strychnine (0.5 μM). V_h, −60 mV. Consecutive traces recorded before and 3 min after application of DA (30 μM). *B* and *C*, cumulative probability distribution of inter-event intervals (*B*) and amplitudes (*C*) of mIPSCs in Ca^{2+}-free solution before (131 events per 10 min period) and during DA application (126 events per 10 min period). In Ca^{2+}-free solution, DA no longer affected the distribution. Inset in *C*: superimposed traces of averaged mIPSCs in control (131 events) and during application of DA (126 events). The mean amplitudes of mIPSCs in control and during DA application were 28.2 and 28.4 pA, respectively. *D*, histograms summarizing the inhibitory effect of DA (30 μM) on the frequency of mIPSCs in Ca^{2+} concentrations of 2.4 and 0 mM. Values for 2.4 mM Ca^{2+} and Ca^{2+}-free solutions were 47.2 ± 2.4 % (*n* = 8) and 5.6 ± 2.4 % (*n* = 7), respectively. The effect in the nominally Ca^{2+}-free solution was not significant (*P* > 0.05).
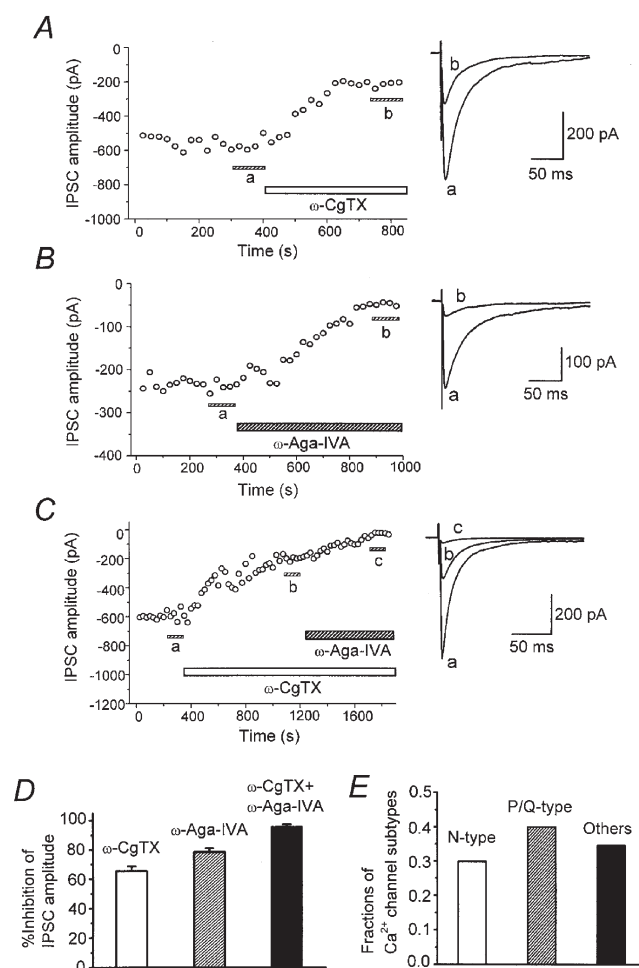
Figure 8. Multiple Ca^{2+} channel subtypes are responsible for inhibitory synaptic transmission onto striatal cholinergic neurones

A–C, time course of the inhibitory effect of ω-CgTX (3 μM) and ω-Aga-IVA (200 nM) on the amplitude of evoked IPSCs (0.2 Hz; V_h, −60 mV). Each point represents the mean amplitude of five consecutive responses. Toxins were bath applied during the indicated periods. Superimposed traces on the right in *A–C* are averages of 20 consecutive IPSCs during the indicated periods. *D*, histograms summarizing the suppression of evoked IPSCs by Ca^{2+} channel blockers. Values for ω-CgTX, ω-Aga-IVA, and both toxins are 65.4 ± 3.3 % (*n* = 11), 78.4 ± 2.7 % (*n* = 7) and 95.9 ± 1.5 % (*n* = 6), respectively. *E*, histograms summarizing the estimated fractions of Ca^{2+} channel subtypes contributing to GABAergic synaptic transmission onto striatal cholinergic neurones. The proportions of N-, P/Q- and other types were 0.298, 0.400 and 0.345, respectively (sum = 1.04), assuming a third power relation between presynaptic Ca^{2+} concentration and postsynaptic response amplitude.

DISCUSSION

The present results suggest that GABAergic afferents to striatal cholinergic interneurones possess presynaptic D_2-like receptors, and that activation of these receptors reduces GABA release by selectively blocking N-type Ca^{2+} channels through an NEM-sensitive pathway, indicative of a PTX-sensitive G protein pathway.

Presynaptic inhibition by D_2-like receptors

We have shown that GABAergic transmission onto striatal cholinergic neurones is inhibited by exogenously applied DA. Our results agree with the recent report by Pisani *et al.* (2000) showing that a D_2-like receptor agonist inhibited GABAergic postsynaptic potentials in striatal cholinergic neurones. To further elucidate the underlying mechanisms, it is an important issue to identify whether the the action of DA is presynaptic or postsynaptic. The most direct approach for this purpose would be to record from presynaptic terminals, which, in practice, is difficult in most synapses due to their small size. Given this limitation, analysis of mIPSCs would be the most useful approach, since it allows examination of presynaptic (frequency) and postsynaptic (amplitude)

parameters separately (Koga & Momiyama, 2000). We unambiguously identified that the action of DA was presynaptic, since DA reduced the frequency of mIPSCs, while the amplitude distribution was unaffected.

In our pharmacological assay, both the agonist and antagonist selective for D_1-like receptors were without effect, at concentrations that were clearly effective at other central synapses (Momiyama *et al.* 1996). In contrast, a D_2-like receptor selective antagonist, sulpiride, exhibited a clear blocking effect on the DA-induced suppression of IPSCs. The affinity of a reversible competitive antagonist (K_B) is independent of the relationship between the response and the receptor occupancy by the agonist, and is thus crucial for identifying the receptor type involved. Our estimate of the K_B value for sulpiride (0.36 μM) was comparable to that for the presynaptic D_2-like receptors on glutamatergic afferents to ventral tegmental DA neurones (Koga & Momiyama, 2000), but was greater (i.e. had lower affinity) than that of cloned D_2-like receptors (Missale *et al.* 1998, 5–50 nM) or D_2-like receptors in dopaminergic neurones of the substantia nigra (Lacey *et*
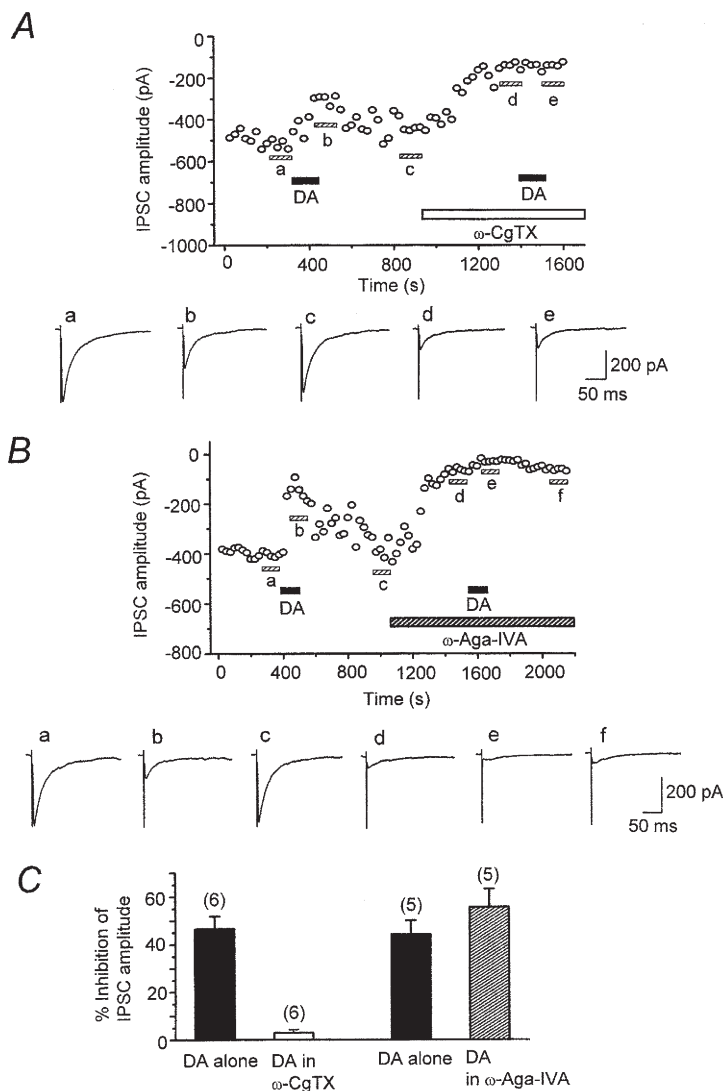
Figure 9. DA-induced inhibition of evoked IPSCs is selectively coupled to N-type Ca^{2+} channels

IPSCs were evoked at 0.2 Hz. V_h, −60 mV. Top panels in *A* and *B*, time course of effects of DA (30 μM) on IPSCs before and after application of ω-CgTX (3 μM, *A*) or ω-Aga-IVA (200 nM, *B*). Each point represents the mean amplitude of five consecutive IPSCs. DA, ω-CgTX and ω-Aga-IVA were applied in the bath during the indicated periods. Toxins were applied after IPSCs had recovered from the inhibition induced by an initial application of DA. After the toxin-induced suppression had reached steady state, DA was applied again. Bottom panels in *A* and *B*, averaged traces of 20 consecutive IPSCs during the indicated periods. *C*, histograms summarizing the effects of ω-CgTX (3 μM) and ω-Aga-IVA (200 nM) on the DA (30 μM)-induced inhibition. After the effect of ω-CgTX had reached steady state, DA no longer affected IPSCs (2.9 ± 1.4 % inhibition, $n = 6$). In contrast, DA still had an effect (55.7 ± 7.6 % inhibition, $n = 5$) after the effect of ω-Aga-IVA had reached steady state. The effects obtained by application of DA alone (44.2 ± 5.9 %, $n = 5$) and DA in the presence of ω-Aga-IVA (55.7 ± 7.6 %, $n = 5$) were not significantly different ($P > 0.05$).

al. 1987, 52 nM). Taken together, the DA-induced inhibition observed in our present study is likely to be mediated by D_2-like receptors, but there may be at least two families of D_2-like receptors with different affinities to sulpiride (5–50 nM and 300–500 nM).

Given the possible diversity of coupled G proteins, their downstream intracellular messages and linked ion channels, a high variation in the coupling efficacy between DA receptors and the responses is expected, even for the same receptor subtype. Thus the difference in the apparent agonist affinity between different synapses (Hsu, 1996; Delgado *et al.* 2000; Koga & Momiyama, 2000; Shen & Johnson, 2000; this study) by itself does not necessarily indicate different DA receptor subtypes. In order to unambiguously identify the presynaptic DA receptor subtypes, future studies using gene targeting strategies will prove to be useful.

Selective blockade of N-type Ca^{2+} channels by DA

The DA-induced inhibition of mIPSC frequency was almost completely abolished in Ca^{2+}-free solution, suggesting that DA reduces mIPSC frequency by inhibiting Ca^{2+} entry at the presynaptic terminal. Such a mechanism has been also shown for presynaptic D_2-like receptor-mediated inhibition of excitatory transmission onto ventral tegmental dopaminergic neurones (Koga & Momiyama, 2000), as well as for D_1-like receptor-mediated presynaptic inhibition of glutamatergic transmission onto magnocellular basal forebrain neurones (Momiyama *et al.* 1996) or GABAergic transmission onto nucleus accumbens neurones (Nicola & Malenka, 1997). Presynaptic regulation of Ca^{2+} entry could be either via a direct effect on Ca^{2+} channels or via an indirect effect through potassium channels. Since the present data have shown that the N-type Ca^{2+} channel selective blocker ω-CgTX specifically blocks the effect of DA, a direct action on presynaptic N-type Ca^{2+} channels is suggested. Because transmitter release and presynaptic Ca^{2+} entry are non-linearly related (Jenkinson, 1957; Dodge & Rahamimoff, 1967; Augustine & Charlton, 1986; Takahashi, 1992), the apparent effect of DA on GABA release can vary, depending on whether the slope of the relationship is steep or shallow. Therefore, it is possible that if blockade of a certain Ca^{2+} channel subtype brings this relationship to a shallow slope range, DA may no longer be effective. However, this was not the case, since DA was still effective when transmission was largely reduced by the P/Q-type Ca^{2+} channel blocker. Suppression of transmission by the N-type Ca^{2+} channel blocker was lower, but DA was no longer effective,

Figure 10. Effect of *N*-ethylmaleimide (NEM) on the DA-induced inhibition of the evoked IPSCs

A, top, time course of the inhibition of IPSCs (0.2 Hz; V_h, −60 mV) by DA (30 μM), which was blocked by NEM (50 μM). Each point represents the mean amplitude of five consecutive IPSCs. DA and NEM were applied in the bath during the indicated periods. After IPSCs had recovered from the initial DA-induced suppression, NEM was applied for 5 min and DA was applied again in the presence of NEM. Bottom, averaged traces of 20 consecutive IPSCs during the indicated periods. *B*, histograms summarizing the effects of DA with and without NEM. DA-induced inhibitory effect in the presence of NEM (6.9 ± 5.2 %, *n* = 6) was significantly (*P* < 0.05) smaller than that of DA alone (44.3 ± 2.2 %, *n* = 6).
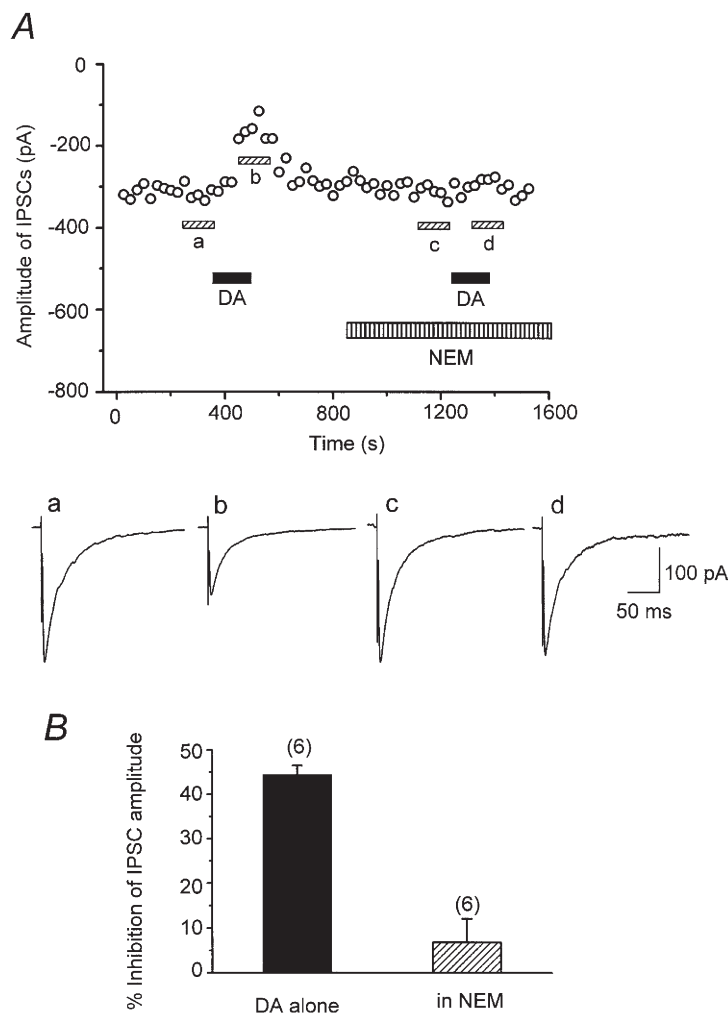
indicating a specific coupling between the action of DA receptors and N-type Ca^{2+} channels. This is the first report that has identified the Ca^{2+} channel subtype involved in DA-induced presynaptic modulation of synaptic transmission. In mammalian central synapses, fast synaptic transmission is mediated by multiple types of high-voltage-activated Ca^{2+} channels, including N-, P/Q- and R-type Ca^{2+} channels (Takahashi & Momiyama, 1993; Wheeler *et al.* 1994). However, the contribution of N-type Ca^{2+} channels is restricted to the early postnatal period in some central synapses (Iwasaki *et al.* 2000). It remains to be seen whether a developmental decrease in N-type Ca^{2+} channels at presynaptic sites occurs at this synapse or not, as well as whether presynaptic inhibition by D_2-like receptors undergoes developmental changes associated with N-type Ca^{2+} channels.

Intracellular pathway in presynaptic terminals

DA receptors belong to a G protein-coupled receptor family (Missale *et al.* 1998). In cultured or acutely dissociated cells, $G_{i/o}$ class G proteins are coupled to the inhibition of Ca^{2+} currents by D_2-like receptors (Lledo *et al.* 1992; Brown & Seabrook, 1995; Yan *et al.* 1997). In the present study, the DA-induced inhibitory effect on IPSCs was significantly suppressed by NEM, a sulfhydryl alkylating agent. Although NEM has been shown to uncouple PTX-sensitive $G_{i/o}$ proteins in rat sympathetic neurones (Shapiro *et al.* 1994), due to the lack of a reliable technique for loading antibodies selective for the $G_{i/o}$ protein subfamily into presynaptic terminals, we have no direct evidence for the involvement of the $G_{i/o}$ class G proteins with presynaptic D_2-like receptors. It is also unknown at present which intracellular messenger systems are involved downstream of the NEM-sensitive G proteins. Recent studies using rat superior cervical ganglion neurones have reported that $G_{i/o}$ class G protein-coupled receptors are capable of inhibiting N-type Ca^{2+} channels through a direct $G_{\beta\gamma}$ subunit signalling pathway (Garcia *et al.* 1998; Ruiz-Velasco & Ikeda, 2000), which might be the most likely scenario in the present study.

Physiological implications

GABAergic inhibitory postsynaptic potentials in striatal cholinergic neurones have been reported to produce a phase-independent prolongation of the interspike interval, and are more likely to influence the overall firing rate of these neurones, whereas excitatory postsynaptic potentials precisely regulate the spike timing (Bennett & Wilson, 1998). A recent study has reported that DA has no effect on glutamatergic postsynaptic potentials evoked by cortical stimulation (Pisani *et al.* 2000). Therefore the present findings suggest that DA could modulate the overall firing of striatal cholinergic neurones through an action on D_2-like receptors located on GABAergic presynaptic terminals.

A number of neurochemical studies have suggested DA-induced modulation of ACh release in the striatum;

activation of D_1-like receptors stimulates ACh release, whereas D_2-like receptor agonists reduce it (for review, see Di Chiara *et al.* 1994). The effects of D_2-like receptor agonists can be readily explained by the fact that the activation of D_2-like receptors on striatal cholinergic neurones inhibits N-type Ca^{2+} currents (Yan *et al.* 1997), since the suppression of Ca^{2+} currents should reduce ACh release. The observations in neurochemical studies are based on experiments where DA was systemically administered, thus including both direct effects on striatal neurones and indirect effects on extrastriatal DA receptors. Our results suggest that inhibitory transmission onto striatal cholinergic neurones is suppressed by the activation of presynaptic D_2-like receptors. This could result in the excitation of cholinergic neurones and therefore may lead to enhanced ACh release in the striatum. There may be other unknown mechanisms that overwhelm such enhanced ACh release, leading to a net inhibition of ACh release by systemic activation of D_2-like receptors.

GABAergic inputs to striatal cholinergic neurones are likely to originate from axon collaterals of striatal medium spiny neurones (Bolam *et al.* 1986; Martone *et al.* 1992) or possibly from GABAergic interneurones (Bennett & Wilson, 1998; Koós & Tepper, 1999). The projection pattern, DA receptor subtypes and neurochemical markers of medium spiny neurones have been reported to be heterogeneous (Gerfen, 2000 and references therein). Despite the presence of such neuronal subpopulations, in all cells we tested (102 out of 102 cells), we observed the suppression of GABAergic transmission via DA receptors. Moreover, data derived from all cells that we examined for DA receptor pharmacology supported the involvement of D_2-like receptors (64 out of 64 cells). One possible scenario that fits with the present data is that all cholinergic neurones receive GABAergic inputs from the neuronal population that expresses D_2-like receptors, the population often found to contain enkephalin (Le Moine & Bloch, 1995; reviewed by Gerfen, 2000). However, given anatomical evidence reporting the frequent contact of GABAergic synapses from substance P-containing medium spiny neurones (the other neuronal population often associated with the expression of D_1-like receptors: Le Moine & Bloch, 1995; Gerfen, 2000) made on cholinergic neurones (Martone *et al.* 1992), the apparent lack of effect of D_1-like receptor-selective drugs may appear somewhat surprising. The puzzle remains even if we adopt another scheme, the colocalization of both D_1- and D_2-like receptors in the same population of medium spiny neurones (Aizman *et al.* 2000). The most straightforward interpretation would be the spatial segregation of the two receptor types: D_1-like receptors are located far from the GABA release site whereas D_2-like receptors are present close to the release site. In addition, a recent report showing that GABA release from medium spiny neurones onto substantia nigra neurones is enhanced by D_1-like receptors (Radnikow &

Misgeld, 1998) suggests that the expression of DA receptor types may be even more diverse and may include target dependency. Thus the identity of the DA receptor type and its function could be differential, between axon collateral terminals and projecting axon terminals. To date, quantitative anatomical identification of GABAergic inputs to striatal cholinergic neurones is not yet available. It also remains to be seen whether the precise subcellular localization of identified DA receptor subtypes expressed in medium spiny neurones can be achieved by use of immuno-electron microscopy.

AIZMAN, O., BRISMAR, H., UHLÉN, P., ZETTERGREN, E., LEVEY, A. I., FORSSBERG, H., GREENGARD, P. & APERIA, A. (2000). Anatomical and physiological evidence for D_1 and D_2 dopamine receptor colocalization in neostriatal neurons. *Nature Neuroscience* **3**, 226–230.

AOSAKI, T., KIUCHI, K. & KAWAGUCHI, Y. (1998). Dopamine D_1-like receptor activation excites rat striatal large aspiny neurons *in vitro*. *Journal of Neuroscience* **18**, 5180–5190.

AUGUSTINE, G. J. & CHARLTON, M. P. (1986). Calcium dependence of presynaptic calcium current and post-synaptic response at the squid giant synapse. *Journal of Physiology* **381**, 619–640.

BENNETT, B. D. & WILSON, C. J. (1998). Synaptic regulation of action potential timing in neostriatal cholinergic interneurons. *Journal of Neuroscience* **18**, 8539–8549.

BENNETT, B. D. & WILSON, C. J. (1999). Spontaneous activity of neostriatal cholinergic interneurons *in vitro*. *Journal of Neuroscience* **19**, 5586–5596.

BERGSON, C., MRZLJAK, L., SMILEY, J. F., PAPPY, M., LEVENSON, R. & GOLDMAN-RAKIC, P. S. (1995). Regional, cellular, and subcellular variations in the distribution of D_1 and D_5 dopamine receptors in primate brain. *Journal of Neuroscience* **15**, 7821–7836.

BOLAM, J. P., INGHAM, C. A., IZZO, P. N., LEVEY, A. I. RYE, D. B., SMITH, A. D. & WAINER, B. H. (1986). Substance P-containing terminals in synaptic contact with cholinergic neurons in the neostriatum and basal forebrain: a double immunocytochemical study in the rat. *Brain Research* **397**, 279–289.

BOLAM, J. P., WAINER, B. H. & SMITH, A. D. (1984). Characterization of cholinergic neurons in the rat neostriatum. A combination of choline acetyltransferase immunocytochemistry, Golgi-impregnation and electron microscopy. *Neuroscience* **12**, 711–718.

BROWN, N. A. & SEABROOK, G. R. (1995). Phosphorylation- and voltage-dependent inhibition of neuronal calcium currents by activation of human $D_{2(short)}$ dopamine receptors. *British Journal of Pharmacology* **115**, 459–466.

CALABRESI, P., CENTONZE, D., GUBELLINI, P., PISANI, A. & BERNARDI, G. (2000). Acetylcholine-mediated modulation of striatal function. *Trends in Neurosciences* **23**, 120–126.

DELGADO, A., SIERRA, A., QUEREJETA, E., VALDIOSERA, R. F. & ACEVES, J. (2000). Inhibitory control of the GABAergic transmission in the rat neostriatum by D_2 dopamine receptors. *Neuroscience* **95**, 1043–1048.

DI CHIARA, G., MORELLI, M. & CONSOLO, S. (1994). Modulatory functions of neurotransmitters in the striatum: ACh/dopamine/NMDA interactions. *Trends in Neurosciences* **17**, 228–233.

DODGE, F. A. & RAHAMIMOFF, R. (1967). Co-operative action of calcium ions in transmitter release at the neuromuscular junction. *Journal of Physiology* **193**, 419–432.

GARCIA, D. E., LI, B., GARCIA-FERREIRO, R. E., HERNANDEZ-OCHOA, E. O., YAN, K., GAUTAM, N., CATTERALL, W. A., MACKIE, K. & HILLE, B. (1998). G-protein β-subunit specificity in the fast membrane-delimited inhibition of Ca^{2+} channels. *Journal of Neuroscience* **18**, 9163–9170.

GERFEN, C. R. (2000). Molecular effects of dopamine on striatal-projection pathways. *Trends in Neurosciences* **23**, suppl. S64–S70.

HSU, K.-S. (1996). Characterization of dopamine receptors mediating inhibition of excitatory synaptic transmission in the rat hippocampal slice. *Journal of Neurophysiology* **76**, 1887–1895.

IWASAKI, S., MOMIYAMA, A., UCHITEL, O. D. & TAKAHASHI, T. (2000). Developmental changes in calcium channel types mediating central synaptic transmission. *Journal of Neuroscience* **20**, 59–65.

JENKINSON, D. H. (1957). The nature of the antagonism between calcium and magnesium ions at the neuromuscular junction. *Journal of Physiology* **138**, 434–444.

JIANG, Z.-G. & NORTH, R. A. (1991). Membrane properties and synaptic responses of rat striatal neurones *in vitro*. *Journal of Physiology* **443**, 533–553.

KANEKO, S., HIKIDA, T., WATANABE, D., ICHINOSE, H., NAGATSU, T., KREITMAN, R. J., PASTAN, I. & NAKANISHI, S. (2000). Synaptic integration mediated by striatal cholinergic interneurons in basal ganglia function. *Science* **289**, 633–637.

KAWAGUCHI, Y. (1992). Large aspiny cells in the matrix of the rat neostriatum *in vitro*: physiological identification, relation to the compartments and excitatory postsynaptic currents. *Journal of Neurophysiology* **67**, 1669–1682.

KAWAGUCHI, Y., WILSON, C. J., AUGOOD, S. J. & EMSON, P. C. (1995). Striatal interneurones: chemical, physiological and morphological characterization. *Trends in Neurosciences* **18**, 527–535.

KOGA, E. & MOMIYAMA, T. (2000). Presynaptic dopamine D_2-like receptors inhibit excitatory transmission onto rat ventral tegmental dopaminergic neurones. *Journal of Physiology* **523**, 163–173.

KOÓS, T. & TEPPER, J. M. (1999). Inhibitory control of neostriatal projection neurons by GABAergic interneurons. *Nature Neuroscience* **2**, 467–472.

KUBOTA, Y., INAGAKI, S., SHIMADA, S., KITO, S., ECKENSTEIN, F. & TOHYAMA, M. (1987). Neostriatal cholinergic neurons receive direct synaptic inputs from dopaminergic axons. *Brain Research* **413**, 179–184.

LACEY, M. G., MERCURI, N. B. & NORTH, R. A. (1987). Dopamine acts on D_2 receptors to increase potassium conductance in neurones of the rat substantia nigra zona compacta. *Journal of Physiology* **392**, 397–416.

LEHMANN, J. & LANGER, S. Z. (1983). The striatal cholinergic interneuron: synaptic target of dopaminergic terminals? *Neuroscience* **10**, 1105–1120.

LE MOINE, C. & BLOCH, B. (1995). D1 and D2 dopamine receptor gene expression in the rat striatum: sensitive cRNA probes demonstrate prominent segregation of D1 and D2 mRNAs in distinct neuronal populations of the dorsal and ventral striatum. *Journal of Comparative Neurology* **355**, 418–426.

LLEDO, P. M., HOMBURGER, V., BOCKAERT, J. & VINCENT, J.-D. (1992). Differential G protein-mediated coupling of D_2 dopamine receptors to K^+ and Ca^{2+} currents in rat anterior pituitary cells. *Neuron* **8**, 455–463.

Martone, M. E., Armstrong, D. M., Young, S. J. & Groves, P. M. (1992). Ultrastructural examination of enkephalin and substance P input to cholinergic neurons within the rat neostriatum. *Brain Research* **594**, 253–262.

Missale, C., Nash, S. R., Robinson, S. W., Jaber, M. & Caron, M. G. (1998). Dopamine receptors: from structure to function. *Physiological Reviews* **78**, 189–225.

Momiyama, T. & Koga, E. (1999). Dopamine-induced presynaptic inhibition of inhibitory transmission onto rat striatal cholinergic neurons. *Society for Neuroscience Abstracts* **25**, 1503.

Momiyama, T., Sim, J. A. & Brown, D. A. (1996). Dopamine D$_1$-like receptor-mediated presynaptic inhibition of excitatory transmission onto rat magnocellular basal forebrain neurones. *Journal of Physiology* **495**, 97–106.

Nicola, S. M. & Malenka, R. C. (1997). Dopamine depresses excitatory and inhibitory synaptic transmission by distinct mechanisms in the nucleus accumbens. *Journal of Neuroscience* **17**, 5697–5710.

Nirenberg, M. J., Vaugham, R. A., Uhl, G. R., Kuhar, M. J. & Pickel, V. M. (1996). The dopamine transporter is localized to dendritic and axonal plasma membranes of nigrostriatal dopaminergic neurons. *Journal of Neuroscience* **15**, 436–447.

Phelps, P. E., Houser, C. R. & Vaughn, J. E. (1985). Immuno-cytochemical localization of choline acetyltransferase within the rat neostriatum: a correlated light and electron microscopic study of cholinergic neurons and synapses. *Journal of Comparative Neurology* **238**, 286–307.

Pisani, A., Bonsi, P., Centonze, D., Calabresi, P. & Bernardi, G. (2000). Activation of D2-like dopamine receptors reduces synaptic inputs to striatal cholinergic interneurons. *Journal of Neuroscience* **20**, RC69 (1–6).

Radnikow, G. & Misgeld, U. (1998). Dopamine D$_1$ receptors facilitate GABA$_A$ synaptic currents in the rat substantia nigra pars reticulata. *Journal of Neuroscience* **18**, 2009–2016.

Ruiz-Velasco, V. & Ikeda, S. R. (2000). Multiple G-protein $\beta\gamma$ combinations produce voltage-dependent inhibition of N-type calcium channels in rat superior cervical ganglion neurons. *Journal of Neuroscience* **20**, 2183–2191.

Shapiro, M. S., Wollmuth, L. P. & Hille, B. (1994). Modulation of Ca^{2+} channels by PTX-sensitive G-proteins is blocked by *N*-ethylmaleimide in rat sympathetic neurons. *Journal of Neuroscience* **14**, 7109–7116.

Shen, K.-Z. & Johnson, S. W. (2000). Presynaptic dopamine D$_2$ and muscarine M$_3$ receptors inhibit excitatory and inhibitory transmission to rat subthalamic neurones *in vitro*. *Journal of Physiology* **525**, 331–341.

Takahashi, T. (1992). The minimal inhibitory synaptic currents evoked in neonatal rat motoneurones. *Journal of Physiology* **450**, 593–611.

Takahashi, T. & Momiyama, A. (1993). Different types of calcium channels mediate central synaptic transmission. *Nature* **366**, 156–158.

Wheeler, D. B., Randall, A. & Tsien, R. W. (1994). Roles of N-type and Q-type Ca^{2+} channels in supporting hippocampal synaptic transmission. *Science* **264**, 107–111.

Yan, Z., Song, W.-J. & Surmeier, D. J. (1997). D$_2$ dopamine receptors reduce N-type Ca^{2+} currents in rat neostriatal cholinergic interneurons through a membrane-delimited, protein-kinase-C-insensitive pathway. *Journal of Neurophysiology* **77**, 1003–1015.

Yan, Z. & Surmeier, D. J. (1997). D$_5$ dopamine receptors enhance Zn^{2+}-sensitive GABA$_A$ currents in striatal cholinergic interneurons through PKA/PP1 cascade. *Neuron* **19**, 1115–1126.

Corresponding author

T. Momiyama: Division of Cerebral Structure, National Institute for Physiological Sciences, Myodaiji, Okazaki 444-8585, Japan.

Email: tmomi@nips.ac.jp